Heliyon 10 (2024) e24809

Contents lists available at ScienceDirect

Heliyon

journal homepage: www.cell.com/heliyon

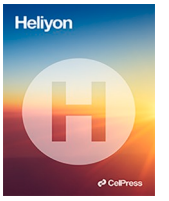

Research article

Animal models of brain and spinal cord metastases of NSCLC established using a brain stereotactic instrument

Xuerou Liu [a], Shiyao Liu [a], Yumei Yang [a], Hui Cai [a], Ruijie Zheng [a], Yaoshuai Zhang [a], Xian Li [a,b], Fangtian Fan [a,b], Hao Liu [a,b,**], Shanshan Li [a,b,*]

[a] School of Pharmacy, Bengbu Medical University, Bengbu, China
[b] Anhui Province Engineering Technology Research Center of Biochemical Pharmaceutical, Bengbu, China

ARTICLE INFO

Keywords:
Animal models
Non-small cell lung cancer
Brain metastasis
Spinal cord metastasis
Brain stereotaxic device

ABSTRACT

Objective: Animal models of brain and spinal cord metastases of non-small cell lung cancer were established through the intracranial injection of PC-9 Luc cells with a brain stereotaxic device. This method provides a reliable modeling method for studying brain and spinal cord metastases of non-small cell lung cancer.

Methods: PC-9 Luc cells at logarithmic growth stage were injected into the skulls of 5-week-old BALB/c nude mice at different cell volumes (30×10^4, 80×10^4) and different locations (using anterior fontanel as a location point, 1 mm from the coronal suture, and 1.5 mm from the sagittal suture on the right upper and right lower side of the skull). After 1 week of cell inoculation, fluorescence signals of tumor cells in the brain and spinal were detected using the IVIS Xenogen Imaging system. After 4 weeks, brain and spinal tissues from the nude mice were harvested. Following paraffin-embedded sectioning, HE staining was performed on the tissues.

Results: The fluorescence signals revealed that both brain and spinal cord metastasis occurred in the mice where the cells were injected at the lower right side of the skull. There was only brain metastasis in the nude mice injected with 30×10^4 cells at the upper right side of the skull. Both brain and spinal cord metastasis occurred in the nude mice injected with 80×10^4 cells. The HE staining revealed that both brain and spinal cord metastasis occurred in the mice injected with different amounts of PC-9 Luc cells, consistent with the results detected using the IVIS Xenogen Imaging system, thereby demonstrating the reliability of detecting fluorescent signals *in vivo* to determine tumor growth.

Conclusion: It is a reliable method to establish the animal model of brain and spinal cord metastases of non-small cell lung cancer by injecting different quantities of cells from different positions with a brain stereotaxic device. The IVIS Xenogen Imaging system has high reliability in detecting the fluorescence signals of brain and spinal cord metastatic tumors.

1. Introduction

According to the latest global cancer statistics analysis, lung cancer is the leading cause of cancer-related death, with approximately

* Corresponding author. School of Pharmacy, Bengbu Medical University, Bengbu, China
** Corresponding author. School of Pharmacy, Bengbu Medical University, Bengbu, China
E-mail addresses: liuhao6886@foxmail.com (H. Liu), lishanshan900122@163.com (S. Li).

https://doi.org/10.1016/j.heliyon.2024.e24809
Received 17 June 2023; Received in revised form 11 January 2024; Accepted 15 January 2024
Available online 20 January 2024

1.8 million people dying from lung cancer worldwide, accounting for approximately 18 % of all cancer-related deaths [1]. Lung cancer consists of non-small and small cell lung cancer, with non-small cell lung cancer comprising approximately 85 % of all cases [2]. Patients with non-small cell lung cancer have a higher risk of central nervous system (CNS) metastases with driver gene activation mutations [3–5]. CNS metastases include brain and spinal cord metastases [6,7]. Brain metastases are the most common intracranial malignancy; most primary tumors originate in the lungs [8,9]. Approximately 10%–15 % of lung cancer patients are initially diagnosed with brain metastases, and approximately 20%–50 % develop brain metastases during the disease progression [10,11].

Spinal cord metastases involve tumors that have metastasized to the spinal cord. With the prolonged survival of tumor patients and the use of MRI and PET in clinical practice, the detection rate of spinal cord metastases has increased, reaching 2%–5% [12]. Spinal cord metastases tend to occur in advanced cancer, and patients usually have brain metastases or systemic metastases [13]. The most prevalent spinal cord metastases are lung cancer, especially non-small cell lung cancer, followed by breast cancer, renal cell carcinoma, melanoma, colorectal cancer, and lymphoma [14]. In a retrospective study of 138 cases of spinal cord metastases previously reported in the literature, spinal cord metastases patients from different primary tumors were analyzed and it was found that 54 % of the spinal cord metastases patients originated from lung cancer [15]. Sung [16] et al. reported 301 patients with spinal cord metastases, 47 % of which originated from lung cancer.

The main hypotheses for the pathogenesis of spinal cord metastases included: 1. arterial haematogenous metastasis; 2. vertebral venous system metastasis; 3. direct metastasis; 4. implantation metastasis. Tumor cells metastasize to the spinal cord via blood vessels, central cerebrospinal fluid ducts, or adjacent tissue invasion [17–19]. Brain tumors often metastasize to the spinal cord via the implantation metastatic pathway and direct diffusion of tumor cells through the central canal of the cerebrospinal fluid to the chondrospinal membrane, followed by dissemination to the spinal cord parenchyma [20]. Spinal cord metastases may cause intractable pain and pathological fracture, leading to spinal instability, and the tumor tissue may further grow and compress the spine, leading to paralysis of the patients, seriously affecting the survival and quality of life of the patients [21,22]. Clinical management of spinal cord metastases includes microsurgical resection, chemotherapy (especially intrathecal chemotherapy), molecularly targeted therapy, hormones and radiotherapy. However, once spinal cord metastases occurs, the disease progresses rapidly and patients often have a poor prognosis, with a median survival of merely 104.5 days [22]. Therefore, it is imperative to strengthen the research on the occurrence and development of spinal cord metastases to provide a theoretical basis for the treatment of spinal cord metastases. The establishment of animal models is a prerequisite for carrying out relevant studies, and the establishment of experimental animal models of lung cancer brain metastases and spinal cord metastases is an important foundation for studying lung cancer brain metastases and spinal cord metastases. However, fundamental research continues lacking stable animal models of spinal cord metastases. Therefore, we need to establish an effective experimental animal model, and the model should have a good repeatability.

The present study used the non-small cell lung cancer cell line PC-9 Luc transfected with luciferase to establish a stable animal model of NSCLC with brain and spinal cord metastases through a brain stereotaxic device. We then detected intracranial and spinal histological features with the IVIS Xenogen Imaging system to clarify whether the modeling was successful. After 4 weeks, the brain and spine tissues of mice were taken, and the tissues were stained with hematoxylin-eosin (HE) to confirm the reliability of this modeling method and to provide a prerequisite for further research on anti-NSCLC brain metastasis and spinal cord metastasis drugs or molecular mechanisms, which is essential for clinical improvement of treatment bottlenecks in patients with brain and spinal cord metastases.

2. Materials

2.1. Cell culture and animals

PC-9 Luc cells were obtained from Saiku Biotechnology Co., Ltd. The cells were cultured in RPMI 1640 medium; the medium was supplemented with 10 % FBS and Hygromycin B solution (200 μg/mL) [23]. The cells were grown in an atmosphere containing 5 % CO_2 at 37 °C. Nude mice were obtained from Changzhou Cavens Laboratory Animal Co., Ltd. and raised in a specific pathogen-free environment.

2.2. Main reagents and instruments

RPMI 1640 medium was obtained from Gibco Life Technologies Co., Ltd., whereas D-Luciferin potassium salt was from APExBIO Technology Co., Ltd. The medical adhesive was purchased from Beijing Kang Paite Medical Equipment Co., Ltd. The IVIS Xenogen Imaging system (FX-PRO, USA) was used to monitor the fluorescent signals. The brain stereotaxic device and drilled needle were purchased from RWD Life Science Co., Ltd.

3. Methods

3.1. Cell bioluminescence detection in vitro

First, the PC-9 Luc cells were continuously cultured and planted in a 60-mm culture plate. When the cell density reached 100 %, the plate was washed twice with PBS. Approximately 2 mL of PBS and 50 μL of D-Luciferin potassium salt (15 mg/mL) were added to the plate. The fluorescence intensity in the culture plate was detected using the IVIS Xenogen Imaging system. The bioluminescence of the cells was monitored once a week for 3 weeks to observe the stability of PC-9 Luc cells' bioluminescence *in vitro*. The PC-9 Luc cells were

then implanted in 48-well plates with varying cell numbers of 5×10^3, 1×10^4, 2×10^4, 5×10^4, 1×10^5, 2×10^5, and 4×10^5. After the cells were plastered, 20 μL of D-Luciferin potassium salt (15 mg/mL) was added to each well. The total photon amount in each well was detected using the IVIS Xenogen Imaging system, and the relationship between cell number and bioluminescence signal was analyzed.

3.2. *Establishment of brain metastasis and spinal cord metastasis models*

The metastasis model was established via the intracranial injection of PC-9 Luc cells into the 5-week-old BALB/c nude mice. The tumor seeding process was conducted on the ultra-clean bench.

Prepared cells: The cell suspension concentrations of PC-9 Luc cells at the logarithmic growth phase were 1×10^8/mL and 2.7×10^8/mL.

Anesthetized nude mice: We used the gas anesthetic isoflurane to anesthetize nude mice.

Opened the brain: The skin of the nude mice was wiped with alcohol cotton, and it was cut approximately 1–2 cm from the top of the skull along the center of the nude mice; the fascia was scrubbed with hydrogen peroxide, and the anterior fontanel was exposed by

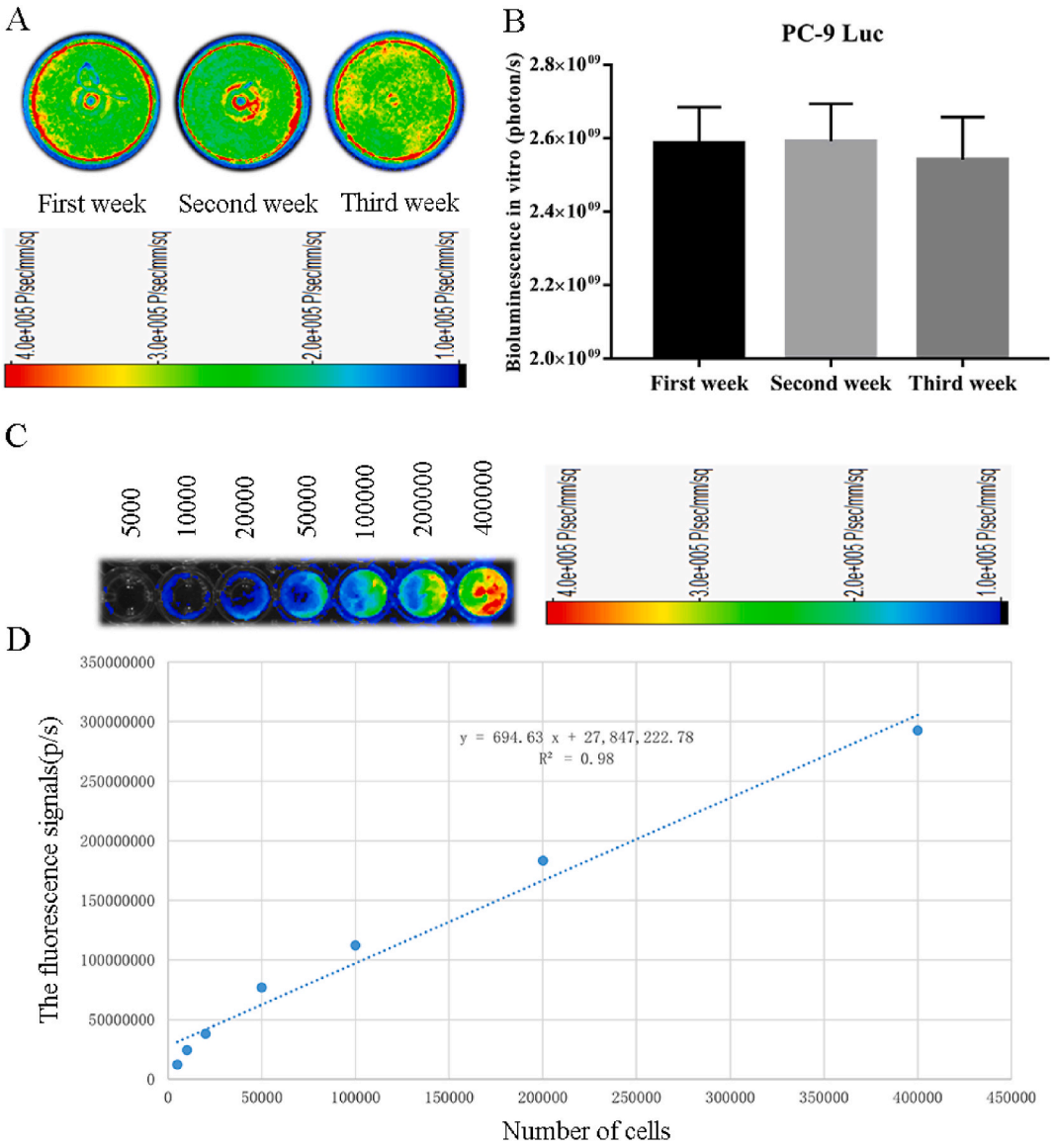

Fig. 1. Cellular bioluminescence over different weeks and different cell numbers *in vitro*. A The image of cellular fluorescence signal intensity in 3 weeks. B The quantification of cellular bioluminescence in A. C The image of cell fluorescence signal intensity with different cell numbers. D The regression equation of fluorescence signal value with different cell numbers.

wiping with a cotton swab.

Bored hole: Using the anterior fontanel as a reference point, we drilled a hole 1 mm from the coronal suture and 1.5 mm from the sagittal suture of the fontanelle on the right upper or right lower side of the skull. The cranial drill centered vertically and drilled slowly to prevent brain injury, and the diameter of the drilled needle is around 0.5 mm.

Injected cells: The experiment was operated on a brain stereotaxic device. The needle tip of the syringe connected to the brain stereotaxic device was aligned with the hole in the skull. The needle depth was first inserted at 3.5 mm down and then 0.5 mm up; The cell injection site is within the brain parenchyma, 3 μL of the cells were injected, and the injection rate was 1 μL/min. The needle was withdrawn after the cells were injected for 1–2 min. The wound was wiped with a cotton swab; the drill hole and the skin wound of nude mice were glued with medical adhesive. The nude mice were placed on an electric blanket and returned to the animal room for further feeding after they had awakened.

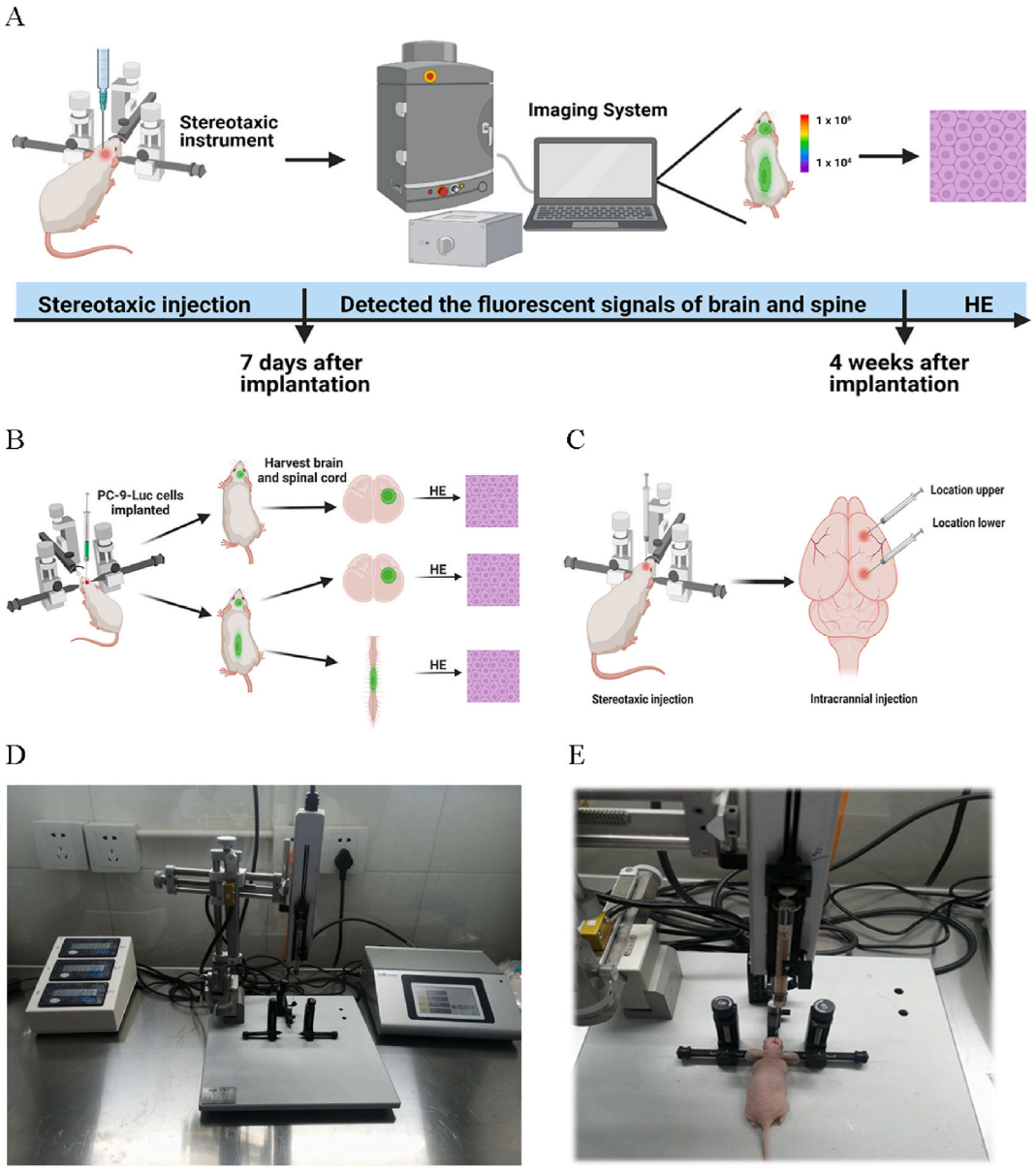

Fig. 2. Process of constructing brain metastasis and spinal cord metastasis models. A, B The flow chart of experimental design. C The location of inoculating PC-9 Luc cells intracranially. D The image of brain stereotaxic device. E The mice were inoculated with cells intracranially by using the brain stereotaxic device.

3.3. Bioluminescence imaging of nude mice

We used the IVIS Xenogen Imaging system to detect the bioluminescent signals to monitor tumor growth in the brain and spine 7 days after the inoculation of PC-9 Luc cells.

3.4. Pathological examination of metastatic lesions in brain and spinal tissues

The brain and spinal tissues from nude mice were collected 4 weeks after intracranial inoculation with PC-9 Luc cells. The tissues were fixed after dehydration, embedded in paraffin, and sectioned for HE staining to observe the presence of tumor metastases in the brain and spine cord.

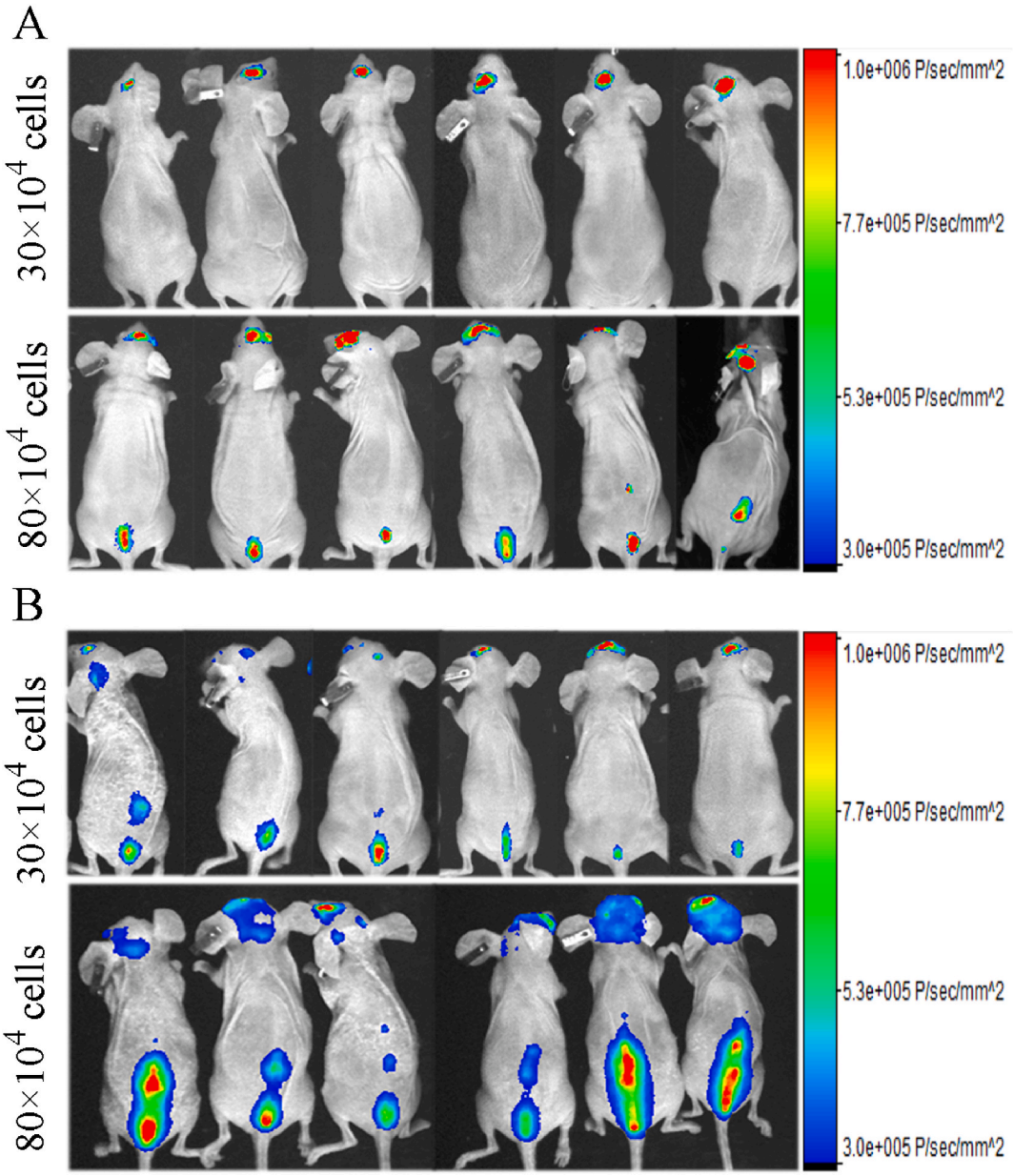

Fig. 3. Fluorescent signals of mice with brain and spinal cord metastases were detected using the IVIS Xenogen Imaging system. A The mice were injected with 30×10^4 and 80×10^4 cells in the upper right side of the anterior fontanelle; B The mice were injected with 30×10^4 and 80×10^4 cells in the lower right side of the anterior fontanelle.

3.5. Statistical analysis

The data were presented as the mean ± SEM, and the date were analyzed by one-way or two-way ANOVA to analyze the difference between groups. P values < 0.05 was considered as significant difference.

4. Results

4.1. Cellular in vitro bioluminescence detection

We used the IVIS Xenogen Imaging system to detect the bioluminescence of cells *in vitro* for 3 weeks. The differences in total photons between the cells were not statistically significant, indicating that the bioluminescence of PC-9 Luc *in vitro* did not decay with cell passages and had desirable bioluminescence stability (Fig. 1A–B). The relationship between fluorescence signal intensity and the number of cells is shown in the figure, and the regression equation of fluorescence signal value (Y) with the number of cells (X) is $Y = 694.63X+27847222.78$, $R^2 = 0.98$, indicating that the fluorescence signal depends on the number of cells and that the relationship is linear (Fig. 1C–D).

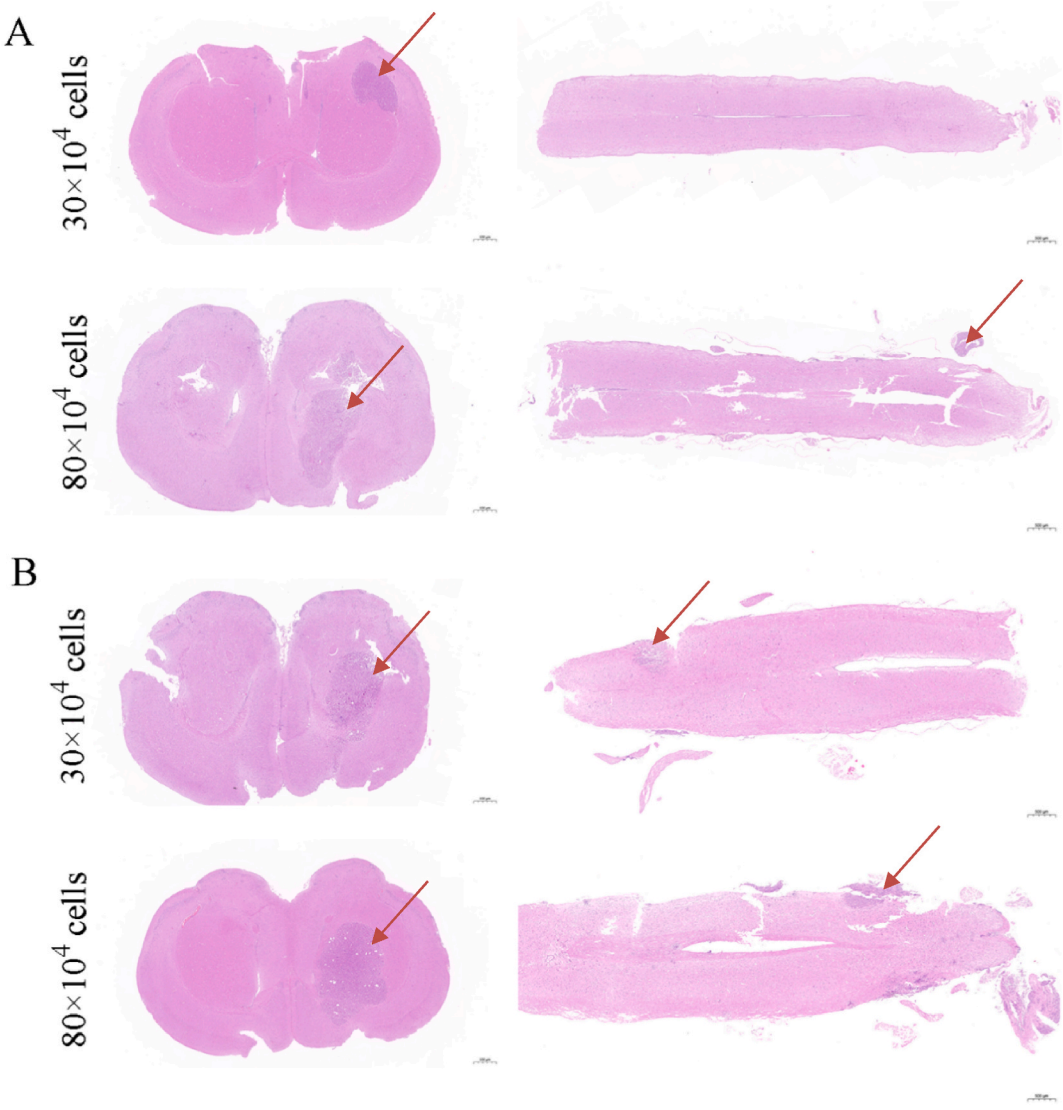

Fig. 4. Pathological examination of brain and spine lesions. A The image with 30×10^4 and 80×10^4 cells in the upper right side of the anterior fontanelle; B The image with 30×10^4 and 80×10^4 cells in the lower right side of the anterior fontanelle.

4.2. Establishment of intracranial brain metastasis and spinal cord metastasis models in mice

We used the brain stereotaxic device to construct brain metastasis and spinal cord metastasis models (Fig. 2A–E).

4.3. The situation of brain and spinal cord metastases was detected in nude mice

The cells were injected in the upper right side of the anterior fontanelle of 1 mm from the coronal suture and 1.5 mm from the sagittal suture. The mice injected with 30×10^4 cells had only brain metastasis, whereas the mice injected with 80×10^4 cells had both brain and spinal cord metastasis (Fig. 3A). The cells were injected in the lower right side of the anterior fontanelle of 1 mm from the coronal suture and 1.5 mm from the sagittal suture of the fontanelle. The mice injected with 30×10^4 and 80×10^4 cells had brain and spinal cord metastasis (Fig. 3B).

4.4. The pathological examination of brain and spine lesions by HE

We performed HE staining of brain and spinal tissues of mice under different treatments, and the results of HE pathology staining showed that at the position of the right upper fontanel, the brain tissues of mice injected with a volume of 30×10^4 cells showed obvious cellular heterogeneity, and the spinal tissues of mice had no obvious cellular heterogeneity, the mice only occurred brain metastasis; mice injected with a volume of 80×10^4 cells showed obvious cellular heterogeneity of the brain and spinal tissues, and not only brain metastasis, but also spinal cord metastasis existed (Fig. 4A).

At the location of the right lower part of the fontanel, both brain and spinal tissues of mice injected with 30×10^4 cells showed significant cellular heterogeneity, with not only brain metastasis but also spinal cord metastasis; mice injected with 80×10^4 cells showed significant cellular heterogeneity, with not only brain metastasis but also spinal cord metastasis occurring (Fig. 4B).

5. Discussion

Brain metastasis from lung cancer is the most prevalent intracranial metastatic malignancy [24]. Brain metastasis is the leading cause of death in lung cancer patients and one of the common causes of treatment failure [25,26], and the patients are often accompanied by neurological dysfunction caused by the occupancy of brain metastases and have inferior quality of life [27,28]. Spinal cord metastasis—also malignant metastasis—is characterized by rapid clinical progression and a poor prognosis [29–32]. Primary tumors that can develop spinal cord metastasis include lung cancer, breast cancer [33], and melanoma [34], etc., with lung cancer being the most prone to spinal cord metastasis [35,36]. At a later stage, patients with spinal cord metastasis show severe pain in the lower back, leading to impaired neurological function, diminished sensory ability, and general weakness [30]. Patients with brain and spinal cord metastases have limited treatment options and a poor prognosis [37–40]; establishing relevant animal models is an essential experimental basis for studying brain and spinal cord metastases from lung cancer.

The current methods for establishing brain metastasis models of lung cancer include intracranial local *in situ* injection, tail vein injection, and left ventricular injection [41], Emilly S Villodre et al. [42] and Daniel L. Smith et al. [43] demonstrated that the tail vein injection method is simple to operate, but it is prone to peripheral organ metastasis and has a low success rate in establishing brain metastasis models. Gong et al. [44] illustrated that the left ventricular injection method is also prone to peripheral metastasis. The occurrence of peripheral metastasis affects the survival quality of animals and interferes with the experimental research results to a certain extent. Our intracranial *in situ* injection has the advantages of a high success rate and low mortality rate and can be used for the pharmacodynamic evaluation of intracranial antitumor drugs [21,45].

Roberto Gazzeri [46] suggested that lung cancer is a common type of cancer that develops intramedullary metastasis of the spinal cord, and spinal cord metastasis is one of the key factors for the poor prognosis of the patients, and its treatment is mainly based on surgical resection, but it is prone to recurrence after the operation; Fabio Volpe [47] suggested in the case report on intramedullary metastasis of differentiated thyroid carcinoma that alleviating the compression of the tumor and resecting the tumor are important means, but the tumor still has the risk of metastasis; Rutula Sonawane [48] suggested that in some patients without sensory pain, the preexisting asymptomatic stage may delay the treatment of the disease and lead to paralysis or even paralysis, therefore, early diagnosis is the key to improve the prognosis of the disease, and in the case of patients with spinal cord metastasis, radiotherapy and surgery are the commonly used means, but there still exists the risk of recurrence, leading to its poor therapeutic effect. At this stage, little has been achieved in treating the progression of spinal cord metastases, and their therapeutic effects remain frustrating. Therefore, there is an urgent need to find new treatment modalities. Animal models are the basis of disease research, and there are few methods to establish experimental animal models of spinal cord metastases, which constrains the basic research of spinal cord metastases. Therefore, there is a need to establish mature experimental animal models of spinal cord metastases to provide more solutions and corresponding experimental basis for clinical treatment of spinal cord metastases.

Imaging techniques such as CT, MRI, ultrasound, and small animal live imaging play an essential role in the basic research of animal tumor models. In this study, an animal live imaging system was used to monitor intracranial and spinal tumor lesions in mice to assess the modeling of brain and spinal cord metastases of lung cancer. This imaging system used bioluminescence technology to monitor the fluorescence signal by converting chemical energy into light energy using the substrate luciferin potassium salt to interact with tumor cells that stably express luciferase, which has a high sensitivity. We also observed the presence of tumor lesions in the brain and spine of mice through HE staining to confirm the reliability of the aforementioned modeling method.

Zhang [49] used PC-9 Luc cells to establish a brain metastasis model of non-small cell lung cancer, and the quantitative

bioluminescence approach was able to more accurately reflect changes in intracranial tumor signaling. In addition, the use of PC-9 Luc cells in a construct to establish a mouse model of brain metastases also allowed for a more intuitive quantification of the tumor load [50]. In this study, the bioluminescence intensity of PC-9 Luc cells *in vitro* revealed an excellent linear relationship with the number of cells. The number of cells did not decay with cell passage, so it had good bioluminescence stability and was suitable for animal modeling. We established brain metastasis and spinal cord metastasis tumor models of non-small cell lung cancer through the intracranial *in situ* injection of PC-9 Luc cells transfected with luciferase through the brain stereotaxic instrument. We used small animal live imaging and HE staining to detect brain and spinal tumor formation in mice to provide a reference for further research on anti-non-small cell lung cancer brain and spinal cord metastases. We used the intracranial fontanelle of mice as the reference point and drilled holes on the right upper side or right lower side of the skull of mice at 1 mm from the coronal suture and 1.5 mm from the sagittal suture of fontanelle and injected different numbers of cells *in situ* through the brain stereotaxic instrument. After injecting the cells into the mice skull, the cells further colonized and proliferated intracranially; then, the cells invaded the soft meningeal space and spread from the spinal venous plexus or entered the spine through the epidural cavity to form spinal cord metastases, thus establishing animal models of brain and spinal cord metastases of non-small cell lung cancer. All of the nude mice that had received an intracranial injection of PC-9 Luc cells through the brain stereotaxic instrument survived, and the survival rate was 100 %. One week after the cells were inoculated, the intracranial fluorescence signals of nude mice were monitored using the small animal live imaging system. When the cell volumes were 30×10^4 at the location of the right upper side of the skull of mice, five nude mice had tumor lesions, and the tumor formation rates were 83.3 %. When the cell volumes were 30×10^4 at the location of the right lower side of the skull of mice and cell volumes were 80×10^4, all nude mice had tumor lesions in their brains and spines. When the cell volumes were 30×10^4, the nude mice were in good condition. When the cell volumes were 80×10^4, the tumor formation was faster; although brain and spinal cord metastases would occur, the tumor focus was significant. The animals would be emaciated in the later stage, which was not conducive to experimental research, so we could relatively reduce the tumor cell number. Furthermore, the tumorigenesis of nude mice is also related to the age of the animals. T cells in nude mice increase with age, and their immune function also enhances, affecting the success rate of tumor inoculation. Therefore, choosing 4–6-week-old nude mice is recommended.

However, this study must be performed in conjunction with the use of the substrate fluorescein potassium salt and a small animal *in vivo* imaging system in order to reflect intracranial tumor signaling changes. The modeling process is also challenging in terms of choosing the cell injection site, the strength of the cranial drill hole, the depth of the needle, and ensuring the survival rate of the mice during the operation, so extensive practice is required to master the technique.

The present model is based on the human tumor cell PC-9 Luc cells, which can better reflect the growth characteristics and drug response characteristics of human tumors compared with mouse Lewis cells. The successful establishment of this animal model is essential for developing new treatments for patients with non-small cell lung cancer brain and spinal cord metastases. It provides theoretical support for developing and evaluating new clinical drugs so that more treatments can be explored to prolong patients' survival and improve their quality of life.

6. Conclusion

It is a reliable method to establish the animal model of brain and spinal cord metastases of non-small cell lung cancer by injecting different quantities of cells from different positions with a brain stereotaxic device. The IVIS Xenogen Imaging system has high reliability in detecting the fluorescence signals of brain and spinal cord metastatic tumors.

Ethics statement

The animal study was reviewed and approved by the Experimental Animal Teaching and Research Committee of Bengbu Medical College (2022–177).

Funding

The work was supported by Leading Backbone Talents Project in Universities in Anhui Province (grant number 202075); Anhui Provincial Key Research and Development Project (grant number 202104g01020017); Excellent scientific research and innovation team of Anhui universities (2022 AH010084); Technology Project Incubation Program (grant number 2020byfy001); Horizontal Project of Bengbu Medical College (2019-BYHX-03); National Natural Science Foundation of China (grant number 81973658, 81873134); National University Students Innovation and Entrepreneurship Project (202210367064).

Data availability statement

The data that support the findings of this study are available on request from the corresponding author.

CRediT authorship contribution statement

Xuerou Liu: Writing – review & editing, Writing – original draft. **Shiyao Liu:** Methodology. **Yumei Yang:** Methodology. **Hui Cai:** Methodology. **Ruijie Zheng:** Methodology. **Yaoshuai Zhang:** Writing – review & editing. **Xian Li:** Conceptualization. **Fangtian Fan:** Data curation. **Hao Liu:** Funding acquisition. **Shanshan Li:** Funding acquisition, Visualization, Conceptualization, Writing – review &

editing.

Declaration of competing interest

The authors declare the following financial interests/personal relationships which may be considered as potential competing interests:Hao Liu reports financial support was provided by Leading Backbone Talents Project in Universities in Anhui Province. Shanshan Li reports financial support was provided by Anhui Provincial Key Research and Development Project. Hao Liu reports financial support was provided by Excellent scientific research and innovation team of Anhui universities. Fangtian Fan reports financial support was provided by Technology Project Incubation Program. Fangtian Fan reports financial support was provided by Horizontal Project of Bengbu Medical College. Fangtian Fan reports was provided by National Natural Science Foundation of China. Shanshan Li reports financial support was provided by National University Students Innovation and Entrepreneurship Project. If there are other authors, they declare that they have no known competing financial interests or personal relationships that could have appeared to influence the work reported in this paper.

References

[1] H. Sung, J. Ferlay, R.L. Siegel, M. Laversanne, I. Soerjomataram, A. Jemal, F. Bray, Global cancer statistics 2020: GLOBOCAN estimates of incidence and mortality worldwide for 36 cancers in 185 countries, CA A Cancer J. Clin. 3 (71) (2021) 209–249, https://doi.org/10.3322/caac.21660. Epub 2021 Feb 4.

[2] S. Srivastava, A. Mohanty, A. Nam, S. Singhal, R. Salgia, Chemokines and NSCLC: emerging role in prognosis, heterogeneity, and therapeutics, Semin. Cancer Biol. 2 (86) (2022) 233–246, https://doi.org/10.1016/j.semcancer.2022.06.010.

[3] Y. Wang, R. Chen, Y. Wa, S. Ding, Y. Yang, J. Liao, L. Tong, G. Xiao, Tumor immune microenvironment and immunotherapy in brain metastasis from non-small cell lung cancer, Front. Immunol. 13 (2022) 829451, https://doi.org/10.3389/fimmu.2022.829451.

[4] W. Zhao, W. Zhou, L. Rong, M. Sun, X. Lin, L. Wang, S. Wang, Y. Wang, Z. Hui, Epidermal growth factor receptor mutations and brain metastases in non-small cell lung cancer, Front. Oncol. 12 (2022) 912505, https://doi.org/10.3389/fonc.2022.912505.

[5] A. Rybarczyk-Kasiuchnicz, R. Ramlau, K. Stencel, Treatment of brain metastases of non-small cell lung carcinoma, Int. J. Mol. Sci. 2 (22) (2021), https://doi.org/10.3390/ijms22020593.

[6] E. Nieblas-Bedolla, J. Zuccato, H. Kluger, G. Zadeh, P.K. Brastianos, Central nervous system metastases, Hematol. Oncol. Clin. N. Am. 1 (36) (2022) 161–188, https://doi.org/10.1016/j.hoc.2021.08.004.

[7] A. Boire, Metastasis to the central nervous system, continuum (minneapolis, minn.) 6 (26) (2020) 1584–1601, https://doi.org/10.1212/CON.0000000000000939.

[8] A. Boire, P.K. Brastianos, L. Garzia, M. Valiente, Brain metastasis, Nat. Rev. Cancer 1 (20) (2020) 4–11, https://doi.org/10.1038/s41568-019-0220-y.

[9] A.S. Achrol, R.C. Rennert, C. Anders, R. Soffietti, M.S. Ahluwalia, L. Nayak, S. Peters, N.D. Arvold, G.R. Harsh, P.S. Steeg, S.D. Chang, Brain metastases, Nat. Rev. Dis. Prim. 1 (5) (2019) 5, https://doi.org/10.1038/s41572-018-0055-y.

[10] W.Y. Chang, Y.L. Wu, P.L. Su, S.C. Yang, C.C. Lin, W.C. Su, The impact of EGFR mutations on the incidence and survival of stages I to III NSCLC patients with subsequent brain metastasis, PLoS One 2 (13) (2018) e0192161, https://doi.org/10.1371/journal.pone.0192161.

[11] S. Jonna, D.S. Subramaniam, Molecular diagnostics and targeted therapies in non-small cell lung cancer (NSCLC): an update, Discov. Med. 148 (27) (2019) 167–170.

[12] J. M D, S. Hoang, F.B. Mesfin, Intramedullary Spinal Cord Tumors, StatPearls, StatPearls Publishing Copyright ©, 2023.

[13] A. Goyal, Y. Yolcu, P. Kerezoudis, M.A. Alvi, W.E. Krauss, M. Bydon, Intramedullary spinal cord metastases: an institutional review of survival and outcomes, Journal of neuro-oncology 2 (142) (2019) 347–354, https://doi.org/10.1007/s11060-019-03105-2.

[14] D. Samartzis, C.C. Gillis, P. Shih, J.E. O'Toole, R.G. Fessler, Intramedullary spinal cord tumors: Part I-epidemiology, pathophysiology, and diagnosis, Global Spine J. 5 (5) (2015) 425–435, https://doi.org/10.1055/s-0035-1549029.

[15] M. Kalayci, F. Cağavi, S. Gül, S. Yenidünya, B. Açikgöz, Intramedullary spinal cord metastases: diagnosis and treatment - an illustrated review, Acta Neurochir. 12 (146) (2004) 1347–1354, https://doi.org/10.1007/s00701-004-0386-1. ; discussion 1354.

[16] W.S. Sung, M.J. Sung, J.H. Chan, B. Manion, J. Song, A. Dubey, A. Erasmus, A. Hunn, Intramedullary spinal cord metastases: a 20-year institutional experience with a comprehensive literature review, World neurosurgery 3–4 (79) (2013) 576–584, https://doi.org/10.1016/j.wneu.2012.04.005.

[17] A.E. Villegas, T.H. Guthrie, Intramedullary spinal cord metastasis in breast cancer: clinical features, diagnosis, and therapeutic consideration, Breast J. 6 (10) (2004) 532–535, https://doi.org/10.1111/j.1075-122X.2004.21531.x.

[18] S.S. Lee, M.K. Kim, S.J. Sym, S.W. Kim, W.K. Kim, S.B. Kim, J.H. Ahn, Intramedullary spinal cord metastases: a single-institution experience, Journal of neuro-oncology 1 (84) (2007) 85–89, https://doi.org/10.1007/s11060-007-9345-z.

[19] R.E. Lieberson, A. Veeravagu, J.M. Eckermann, J.R. Doty, B. Jiang, R. Andrews, S.D. Chang, Intramedullary spinal cord metastasis from prostate carcinoma: a case report, J. Med. Case Rep. 6 (2012) 139, https://doi.org/10.1186/1752-1947-6-139.

[20] X. Liu, M. Li, G. Chen, Intradural spinal seeding metastasis of clival chordoma: a case report, Transl. Cancer Res. 9 (11) (2022) 3426–3433, https://doi.org/10.21037/tcr-22-211.

[21] Y. Zhang, Y. Zhang, W. Niu, X. Ge, F. Huang, J. Pang, X. Li, Y. Wang, W. Gao, F. Fan, S. Li, H. Liu, Experimental study of almonertinib crossing the blood-brain barrier in EGFR-mutant NSCLC brain metastasis and spinal cord metastasis models, Front. Pharmacol. 12 (2021) 750031, https://doi.org/10.3389/fphar.2021.750031.

[22] K. Wang, L. Jiang, A. Hu, C. Sun, L. Zhou, Y. Huang, Q. Chen, J. Dong, X. Zhou, F. Zhang, Vertebral-specific activation of the CX3CL1/ICAM-1 signaling network mediates non-small-cell lung cancer spinal metastasis by engaging tumor cell-vertebral bone marrow endothelial cell interactions, Theranostics 4 (11) (2021) 4770–4789, https://doi.org/10.7150/thno.54235.

[23] T. Higuchi, H. Oshiro, Z. Zhang, K. Miyake, N. Sugisawa, Y. Katsuya, N. Yamamoto, K. Hayashi, H. Kimura, S. Miwa, K. Igarashi, M. Zhao, M. Bouvet, S.R. Singh, H. Tsuchiya, R.M. Hoffman, Osimertinib regresses an EGFR-mutant cisplatinum- resistant lung adenocarcinoma growing in the brain in nude mice, Translational oncology 4 (12) (2019) 640–645, https://doi.org/10.1016/j.tranon.2019.01.007.

[24] W. Liu, C.A. Powell, Q. Wang, Tumor microenvironment in lung cancer-derived brain metastasis, Chin. Med. J. 5 (135) (2022) 1781–1791, https://doi.org/10.1097/CM9.0000000000002127.

[25] S.T. Jünger, D. Reinecke, A.K. Meissner, R. Goldbrunner, S. Grau, Resection of symptomatic non-small cell lung cancer brain metastasis in the setting of multiple brain metastases, J. Neurosurg. 6 (136) (2021) 1–7, https://doi.org/10.3171/2021.7.JNS211172.

[26] N. Hatton, R. Samuel, M. Riaz, C. Johnson, S.L. Cheeseman, M. Snee, A study of non small cell lung cancer (NSCLC) patients with brain metastasis: a single centre experience, Cancer treatment and research communications 34 (2023) 100673, https://doi.org/10.1016/j.ctarc.2022.100673.

[27] L. Sudmeier, S. Tian, K.A. Higgins, Multidisciplinary management of brain metastases from non-small cell lung cancer in the era of immunotherapy, Curr. Treat. Options Oncol. 9 (22) (2021) 77, https://doi.org/10.1007/s11864-021-00871-y.

[28] H. Gafer, Q. de Waard, A. Compter, M. van den Heuvel, Rapid regression of neurological symptoms in patients with metastasised ALK+ lung cancer who are treated with lorlatinib: a report of two cases, BMJ Case Rep. 7 (12) (2019), https://doi.org/10.1136/bcr-2018-227299.

[29] N. Jayakumar, H. Ismail, S. Athar, N. Ashwood, Perineural invasion in intramedullary spinal cord metastasis, Ann. R. Coll. Surg. Engl. 5 (102) (2020) e94–e96, https://doi.org/10.1308/rcsann.2020.0009.

[30] S. Patnaik, J. Turner, P. Inaparthy, W.K. Kieffer, Metastatic spinal cord compression, Br. J. Hosp. Med. 4 (81) (2020) 1–10, https://doi.org/10.12968/hmed.2019.0399.
[31] A. Amelot, L.M. Terrier, G. Cognacq, V. Jecko, B. Marlier, R. Seizeur, E. Emery, L. Bauchet, V. Roualdes, J. Voirin, C. Joubert, E. Mandonnet, L. Lemnos, B. Mathon, P.J. Le Reste, A. Coca, A. Petit, V. Rigau, K. Mokhtari, A. Rousseau, P. Metellus, D. Figarella-Branger, G. Gauchotte, K. Farah, J. Pallud, I. Zemmoura, Natural history of spinal cord metastasis from brain glioblastomas, Journal of neuro-oncology 2 (162) (2023) 373–382, https://doi.org/10.1007/s11060-023-04298-3.
[32] M. Pojskić, K.I. Arnautović, Microsurgical resection of lung carcinoma spinal cord metastasis: 2-dimensional operative video, Operative neurosurgery (Hagerstown, Md.) 4 (18) (2020) E115–e116, https://doi.org/10.1093/ons/opz167.
[33] G. Scalia, R. Costanzo, A. Viola, L. Bonosi, M. Porzio, A. Giovannini, F. Graziano, D.G. Iacopino, R. Maugeri, G.F. Nicoletti, G.E. Umana, Intramedullary spinal cord metastases from breast cancer: a systematic review, Anticancer Res. 2 (43) (2023) 523–535, https://doi.org/10.21873/anticanres.16189.
[34] H. Mizuta, K. Namikawa, K. Nakama, N. Yamazaki, Intramedullary spinal cord metastasis of malignant melanoma:Two cases with rim signs in contrast-enhanced magnetic resonance imaging: a case report, Molecular and clinical oncology 3 (14) (2021) 47, https://doi.org/10.3892/mco.2021.2209.
[35] I. Nurdillah, I.H. Rizuana, S.O. Syazarina, Spinal schwannomatosis mimicking metastatic extramedullary spinal tumor, Diagnostics 7 (13) (2023), https://doi.org/10.3390/diagnostics13071254.
[36] M. Dankner, S. Lam, T. Degenhard, L. Garzia, M.C. Guiot, K. Petrecca, P.M. Siegel, The underlying biology and therapeutic vulnerabilities of leptomeningeal metastases in adult solid cancers, Cancers 4 (13) (2021), https://doi.org/10.3390/cancers13040732.
[37] R. Medikonda, A. Pant, M. Lim, Immunotherapy as a new therapeutic approach for brain and spinal cord tumors, Adv. Exp. Med. Biol. 1394 (2023) 73–84, https://doi.org/10.1007/978-3-031-14732-6_5.
[38] Y. Han, X. Zhang, Y. Lu, Y. Dong, H. Fu, B. Zhang, Y. Gao, Elemene treatment for NSCLC with multiple CNS metastases: a case report and literature review, OncoTargets Ther. 11 (2018) 6377–6382, https://doi.org/10.2147/OTT.S160970.
[39] A. Sahgal, S.D. Myrehaug, S. Siva, G.L. Masucci, P.J. Maralani, M. Brundage, J. Butler, E. Chow, M.G. Fehlings, M. Foote, Z. Gabos, J. Greenspoon, M. Kerba, Y. Lee, M. Liu, S.K. Liu, I. Thibault, R.K. Wong, M. Hum, K. Ding, W.R. Parulekar, Stereotactic body radiotherapy versus conventional external beam radiotherapy in patients with painful spinal metastases: an open-label, multicentre, randomised, controlled, phase 2/3 trial, the Lancet, Oncology 7 (22) (2021) 1023–1033, https://doi.org/10.1016/S1470-2045(21)00196-0.
[40] H.K. Shin, M. Kim, S. Lee, J.J. Lee, D. Park, S.R. Jeon, S.W. Roh, J.H. Park, Surgical strategy for metastatic spinal tumor patients with surgically challenging situation, Medicine 27 (101) (2022) e29560, https://doi.org/10.1097/MD.0000000000029560.
[41] X. Le, M. Nilsson, J. Goldman, M. Reck, K. Nakagawa, T. Kato, L.P. Ares, B. Frimodt-Moller, K. Wolff, C. Visseren-Grul, J.V. Heymach, E.B. Garon, Dual EGFR-VEGF pathway inhibition: a promising strategy for patients with EGFR-mutant NSCLC, J. Thorac. Oncol. : official publication of the International Association for the Study of Lung Cancer 2 (16) (2021) 205–215, https://doi.org/10.1016/j.jtho.2020.10.006.
[42] E.S. Villodre, X. Hu, B.L. Eckhardt, R. Larson, L. Huo, E.C. Yoon, Y. Gong, J. Song, S. Liu, N.T. Ueno, S. Krishnamurthy, S. Pusch, D. Tripathy, W.A. Woodward, B. G. Debeb, NDRG1 in aggressive breast cancer progression and brain metastasis, J. Natl. Cancer Inst. 4 (114) (2022) 579–591, https://doi.org/10.1093/jnci/djab222.
[43] D.L. Smith, B.G. Debeb, P. Diagaradjane, R. Larson, S. Kumar, J. Ning, L. Lacerda, L. Li, W.A. Woodward, Prophylactic cranial irradiation reduces the incidence of brain metastasis in a mouse model of metastatic, HER2-positive breast cancer, Genes & cancer 12 (2021) 28–38, https://doi.org/10.18632/genesandcancer.212, eCollection 2021.
[44] X. Gong, Z. Hou, M.P. Endsley, E.I. Gronseth, K.R. Rarick, J.M. Jorns, Q. Yang, Z. Du, K. Yan, M.L. Bordas, J. Gershan, P. Deepak, A. Geethadevi, P. Chaluvally-Raghavan, Y. Fan, D.R. Harder, R. Ramchandran, L. Wang, Interaction of tumor cells and astrocytes promotes breast cancer brain metastases through TGF-β2/ANGPTL4 axes, npj Precis. Oncol. 3 (2019) 24, https://doi.org/10.1038/s41698-019-0094-1, eCollection 2019.
[45] Y. Zhang, Y. Li, Y. Han, M. Li, X. Li, F. Fan, H. Liu, S. Li, Experimental study of EGFR-TKI aumolertinib combined with ionizing radiation in EGFR mutated NSCLC brain metastases tumor, Eur. J. Pharmacol. 945 (2023) 175571, https://doi.org/10.1016/j.ejphar.2023.175571.
[46] R. Gazzeri, S. Telera, M. Galarza, G.M. Callovini, S. Isabella, A. Alfieri, Surgical treatment of intramedullary spinal cord metastases: functional outcome and complications-a multicenter study, Neurosurg. Rev. 6 (44) (2021) 3267–3275, https://doi.org/10.1007/s10143-021-01491-8.
[47] F. Volpe, L. Piscopo, M. Manganelli, M. Falzarano, F. Volpicelli, C. Nappi, M. Imbriaco, A. Cuocolo, M. Klain, Intramedullary spinal cord metastases from differentiated thyroid cancer, a case report, Life 6 (12) (2022), https://doi.org/10.3390/life12060863.
[48] R. Sonawane, A. Ghoshal, A. Damani, M. Muckaden, J.K. Deodhar, Intramedullary spinal cord metastases of malignant melanoma: a rare case report on paraplegia in palliative care, Indian J. Palliat. Care 3 (25) (2019) 468–470, https://doi.org/10.4103/IJPC.IJPC_163_18.
[49] S.R. Zhang, L.C. Zhu, Y.P. Jiang, J. Zhang, R.J. Xu, Y.S. Xu, B. Xia, S.L. Ma, Efficacy of afatinib, an irreversible ErbB family blocker, in the treatment of intracerebral metastases of non-small cell lung cancer in mice, Acta Pharmacol. Sin. 2 (38) (2017) 233–240, https://doi.org/10.1038/aps.2016.107.
[50] X. Qi, Y. Zhao, S. Yang, Y. Sun, H. Liu, P. Liu, S. Feng, H. Tui, Z. Yuan, J. Yang, H. Bu, Combined effects of programmed cell death-1 blockade and endostar on brain metastases of lung cancer, Anti Cancer Agents Med. Chem. 6 (23) (2023) 709–716, https://doi.org/10.2174/1871520622666220827125929.